SCIENCE CHINA Materials ARTICLES

mater.scichina.com link.springer.com

Published online 25 January 2018 | https://doi.org/10.1007/s40843-017-9207-2
Sci China Mater 2018, 61(7): 985–992

Near UV-pumped yellow-emitting $Sr_9MgLi(PO_4)_7:Eu^{2+}$ phosphor for white-light LEDs

Jianwei Qiao, Zhiguo Xia*, Zhichao Zhang, Bintao Hu and Quanlin Liu

ABSTRACT **Laboratory discovery of new phosphors for white-light light-emitting diodes (WLEDs) is still an imperative challenge. A new yellow-emitting $Sr_9MgLi(PO_4)_7:Eu^{2+}$ phosphor was discovered based on the mineral-inspired prototype evolution and new phase construction strategy proposed by our group. $Sr_9MgLi(PO_4)_7:Eu^{2+}$ has been synthesized by using a high temperature solid-state method, and its phase structure and luminescence properties have been investigated in detail, and applied in WLED lamp. $Sr_9MgLi(PO_4)_7$ phase is derived from the β-$Ca_3(PO_4)_2$-type mineral structure. Upon 365 nm UV light excitation, the $Sr_9MgLi(PO_4)_7:Eu^{2+}$ phosphor exhibits a broad emission band from 450 nm to 700 nm. The white-light LED lamp was fabricated based on the phosphor blends of the composition-optimized yellow-emitting $Sr_9MgLi(PO_4)_7:Eu^{2+}$ and commercial blue-emitting $BaMgAl_{10}O_{17}:Eu^{2+}$, and a 365 nm UV chip was used as the excitation source. The R_a, CCT value and CIE of the as-fabricated LEDs were found to be 83, 5,612 K, and (0.324, 0.358), respectively. All the results indicate that $Sr_9MgLi(PO_4)_7:Eu^{2+}$ could be potential in the development of UV-pumped white-light LEDs.**

Keywords: phosphor, luminescence, rare earth, LEDs

INTRODUCTION

Rare earth (RE) doped photoluminescence materials have been utilized in many different fields including lighting, lasers, displays, biomedicines, and so on, because of their abundant energy levels transitions over a wide range of photon energies [1–3]. This motivates the search for novel RE materials for emerging applications. Recently, phosphor-converted white light-emitting diodes (pc-WLEDs) have attracted much attention due to their high energy efficiency, high material stability, long operational lifetime and environmentally friendly characteristics [4–7]. Typically, the commercial pc-WLEDs are a combination of a blue-emitting InGaN chip and yellow-emitting $Y_3Al_5O_{12}:Ce^{3+}$ (YAG:Ce^{3+}) phosphors [8]. However, the lacking of red spectral contribution in YAG:Ce^{3+} phosphors leads to a poor color-rendering index (R_a<75) and a high correlated color temperature (CCT>7,000 K) [9,10]. To compensate the lacking of red components, red-emitting phosphors or quantum dots have been studied and applied in WLEDs, such as $K_2SiF_6:Mn^{4+}$ phosphors and $CsPbBr_3$ quantum dots [11,12]. Another alternative way to overcome those disadvantages is to combine the near-ultraviolet (n-UV) LED chip with blue and yellow phosphors [4]. To create pc-WLEDs with high quality photoluminescence properties, much effort has been devoted to phosphors in different host systems.

Recently, our group has proposed a useful method for the discovery of new LED phosphors by mineral-inspired prototype evolution and new phase construction, and it has been used in many different systems [4]. Among them, β-$Ca_3(PO_4)_2$-type compounds have prompted remarkable attention as phosphor host materials because of their versatile structural types and abundant occupation sites for activators [13,14]. There are five independent cationic crystallographic sites in β-$Ca_3(PO_4)_2$ host and the coordination number is as follows: Ca(1) is 7-coordinated, Ca(2) and Ca(3) is 8-coordinated, Ca(4) is 3-coordinated, and Ca(5) is 6-coordinated [15]. A large number of β-$Ca_3(PO_4)_2$-type structure phosphors like $Ca_{10}M(PO_4)_7:Eu^{2+}$ (M=Li, Na and K) [16–19], $Ca_9R(PO_4)_7:Eu^{2+}$ (R=Cr and Rare earth), $Ca_8MgRE(PO_4)_7:Eu^{2+}$ [20–23], $Sr_8MgRE(PO_4)_7:Eu^{2+}$ (RE=Y, La, Gd, Sc) [24–26] have been reported with favorable luminescence properties and versatile applications.

Inspired by the above knowledge, we designed a new yellow-emitting $Sr_9MgLi(PO_4)_7:Eu^{2+}$ phosphor for white light LEDs. In this study, luminescence properties including reflectance spectra and decay time, and thermal stability were discussed in detail. Moreover, a white pc-

The Beijing Municipal Key Laboratory of New Energy Materials and Technologies, School of Materials Sciences and Engineering, University of Science and Technology Beijing, Beijing 100083, China
* Corresponding author (email: xiazg@ustb.edu.cn)

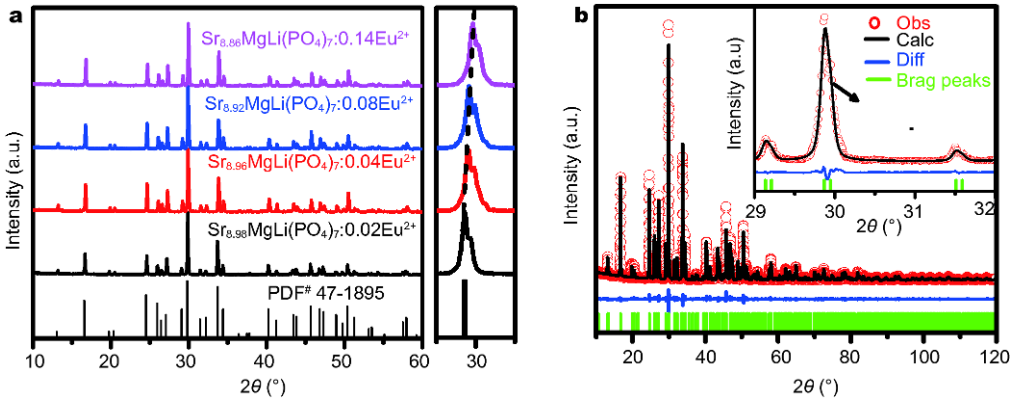

Figure 1 Powder XRD patterns of $Sr_{9-x}MgLi(PO_4)_7:xEu^{2+}$ (x=0.02, 0.04, 0.08 and 0.014) samples (a), and Rietveld profile fitting refinement of the selected sample $Sr_{8.98}MgLi(PO_4)_7:0.02Eu^{2+}$ (b).

WLED device was successfully fabricated by combining the blue-emitting $BaMgAl_{10}O_{17}:Eu^{2+}$ and yellow-emitting $Sr_9MgLi(PO_4)_7:Eu^{2+}$ phosphors with a 365 nm UV chip, and its electroluminescence properties was also reported. All of the results indicate that the $Sr_9MgLi(PO_4)_7:Eu^{2+}$ phosphor can serve as a potential candidate for UV WLEDs.

EXPERIMENTAL SECTION

Materials and synthesis

$Sr_{9-x}MgLi(PO_4)_7:xEu^{2+}$ ($0.02 \leq x \leq 0.14$) phosphors were synthesized *via* a high temperature solid-state route. The stoichiometric mixtures of $SrCO_3$ (99.9%), Li_2CO_3 (99.9%), $(NH_4)_2HPO_4$ (99%), $Mg(OH)_2{\cdot}4MgCO_3{\cdot}6H_2O$ (AR), Eu_2O_3 (99.99%) were ground together with a small amount of ethanol using an agate mortar and pestle until the mixtures were almost dry (25 min). Mixtures were shifted to the crucible and preheated at 800°C for 3 h, and then were sintered under a reducing atmosphere (5% H_2/95% N_2) at 1,300°C for 4 h. After firing, the sintered samples were cooled to room temperature and finely ground with a mortar for further characterization.

Characterization

The powder X-ray diffraction (XRD) data were collected on an X-ray diffractometer (Bruker D8 Advance) with Cu Kα radiation (λ=1.5406 Å) operating at 40 kV and 40 mA. The morphology and microstructure of the samples were examined using a scanning electron microscope (SEM, JEOL JSM-6510A). The photographs of microcrystal particle were obtained by a Nikon $LV_{100}ND$ optical microscope. The photoluminescence (PL), photoluminescence excitation (PLE) and temperature dependent luminescence spectra were measured using a Hitachi F-4600 spectrometer equipped with a photomultiplier tube operating at 400 V and a 150 W Xe lamp as the excitation source. The diffuse reflectance spectra were measured on a Hitachi UH4150 ultraviolet-visible-near infrared spectrophotometer. The decay curves were recorded using a spectrophotometer (Edinburgh Instruments, FLS920) equipped with an *n*F900 flash lamp as the excitation source. The electroluminescence spectra, color temperature (CCT) and color-rendering index (R_a) of the as-fabricated w-LEDs were measured using a UV-vis-near IR spectrophotocolorimeter (PMS-80, Everfine).

RESULTS AND DISCUSSION

Structure of $Sr_9MgLi(PO_4)_7:Eu^{2+}$ phosphor

The XRD patterns of the as-obtained $Sr_{9-x}MgLi(PO_4)_7:xEu^{2+}$ phosphors with various Eu^{2+} doping concentration (x=0.02, 0.04, 0.08, 0.14) are depicted in Fig. 1a. All of the diffraction peaks can be well-indexed to the standard card (PDF 47-1895) of $(Sr_{0.86}Mg_{0.14})_3(PO_4)_2$ phase, which indicates that $Sr_{9-x}MgLi(PO_4)_7:xEu^{2+}$ may be a pure phase iso-structural to $(Sr_{0.86}Mg_{0.14})_3(PO_4)_2$ with the space group of *R*3*c* [27]. According to the enlarged view around 30 degree, the XRD peaks of the series samples shift to larger angle with increasing of Eu^{2+} ions since the ionic radius of Eu^{2+} is smaller than that of Sr^{2+}. TOPAS 4.2 program was used for the Rietveld profile fitting refinement of the selected sample to confirm the phase purity [28]. The Rietveld refinement results revealed that $Sr_9MgLi(PO_4)_7:Eu^{2+}$ has a β-$Ca_3(PO_4)_2$-type structure with space group of *R*3*c*, and the lattice parameters are $a=b$=10.608 Å, c=39.356 Å, $\alpha=\beta$=90°, γ=120°, Z=2, V=3,835.269 Å^3. Unfortunately, we failed to solve the real crystal structure

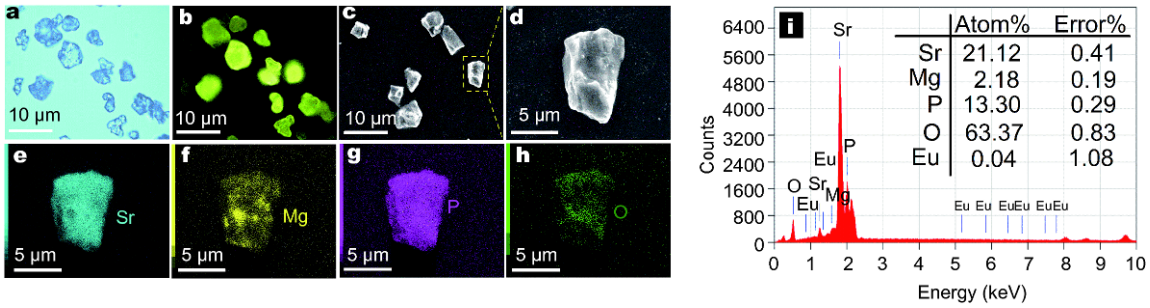

Figure 2 Optical microscope photographs of the $Sr_9MgLi(PO_4)_7:Eu^{2+}$microcrystal particles without (a) and with 365 nm UV excitation (b). SEM images of the $Sr_9MgLi(PO_4)_7:Eu^{2+}$microcrystal particles (c) and the enlarged one particle (d), element mapping images of Sr (e), Mg (f), P (g), and O (h) for the selected $Sr_9MgLi(PO_4)_7:Eu^{2+}$particle, and EDX spectrum and content of $Sr_9MgLi(PO_4)_7:Eu^{2+}$ (i).

because of the splitting at the strongest peak (the inset of Fig. 1b). However, this flaw could not prevent the result on the β-$Ca_3(PO_4)_2$-type structure, and the further studies on the outstanding luminescent properties of $Sr_9MgLi(PO_4)_7:Eu^{2+}$ phosphors, which will be discussed later.

Fig. 2a and b give the optical microscope photographs of $Sr_9MgLi(PO_4)_7:Eu^{2+}$ particles without and with 365 nm UV light source excitation, respectively, and the bright yellow emission in Fig. 2b also predicted the excellent luminescence properties of $Sr_9MgLi(PO_4)_7:Eu^{2+}$ phosphors. Fig. 2c and d demonstrate the SEM images of the $Sr_9MgLi(PO_4)_7:Eu^{2+}$ particles with different scales, and it is found that the microcrystals have well crystallinity with smooth surfaces. The elemental mapping images in Fig. 2e–h and the EDX spectrum in Fig. 2i prove that the presence of Sr, Mg, P, O and Eu elements in $Sr_9MgLi(PO_4)_7:Eu^{2+}$ phosphor. However, Li element was not detected by the elemental mapping because of its small atomic mass. In addition, the detected mole ratio for Sr, Mg, P, O elements approximately equal to 9:0.93:5.7:27, which is close to the stoichiometric ratio of $Sr_9MgLi(PO_4)_7$. Moreover, both the optical microscopy and SEM images in Fig. 2 show that the particle sizes of the as-prepared samples were in the micrometer range with uniform size distribution, which also benefits the fabrication for white LEDs devices.

Luminescence properties of $Sr_9MgLi(PO_4)_7:Eu^{2+}$ phosphors

The UV-vis diffuse reflectance spectra of undoped-$Sr_9MgLi(PO_4)_7$ and $Sr_{9-x}MgLi(PO_4)_7:xEu^{2+}$ (x=0.02, 0.04, 0.08 and 0.14) samples are shown in Fig. 3a. The decreasing reflectance of $Sr_9MgLi(PO_4)_7$ (black solid line) from 200 to 350 nm is ascribed to the host absorption. As a contrast, $Sr_9MgLi(PO_4)_7:Eu^{2+}$ shows a broad band from 250 to 450 nm attributing to the 4f-5d absorption of Eu^{2+}. The band gap of $Sr_9MgLi(PO_4)_7$ can be determined according to the Kubelka-Munk method and Tauc plot [29]. As displayed in the inset of Fig. 3a, the band gap is estimated to be 3.5 eV by extrapolating the linear portion to the photon energy axis.

Fig. 3b and c show the PLE and PL spectra of $Sr_{9-x}MgLi(PO_4)_7:xEu^{2+}$ ($0.02 \le x \le 0.14$) phosphors. As can be seen from the Fig. 3b, the PLE spectra display a broad absorption band from 250 to 450 nm corresponding to the diffuse reflectance spectra. The PL spectra excited by 365 nm light are shown in Fig. 3c. A broad emission band from 450 to 700 nm is indicative of electron transitions from 5d excited state to 4f ground state of Eu^{2+}. Furthermore, the PL spectra can be at least fitted into three bands using Gauss simulation (green dashed line) attributing to the different occupation of Eu^{2+} ions in β-$Ca_3(PO_4)_2$-type phosphor. According to our previous report on $Ca_{10}M(PO_4)_7:Eu^{2+}$ (M = Li, Na and K) phosphors [15], Eu^{2+} ions will occupy parts of the cations' sites. Thus, we can deduce that Eu^{2+} may occupy the Sr1, Sr2 and Sr3 sites equally in $Sr_9MgLi(PO_4)_7:Eu^{2+}$ phosphor. Moreover, with the increase of the Eu^{2+} concentration, the emission intensity increases and reaches a maximum at x=0.04, and then decreases due to the concentration quenching. The concentration quenching occurs mainly because of the non-radiative energy transfers between Eu^{2+} ions within a certain distance. To have a better understanding of the concentration quenching mechanism, the critical distance (R_C) is evaluated using the following equation [30]:

$$R_C = 2\left[\frac{3V}{4\pi X_C N}\right], \quad (1)$$

where X_C is the critical concentration of activator ions; N is the number of cations which can be substituted by the dopant in per unit cell; and V is the volume of the unit cell. In the case of $Sr_{9-x}MgLi(PO_4)_7:xEu^{2+}$ phosphors, X_C = 0.04, V = 3,835.269 Å^3, N = 18. The value of R_C is cal-

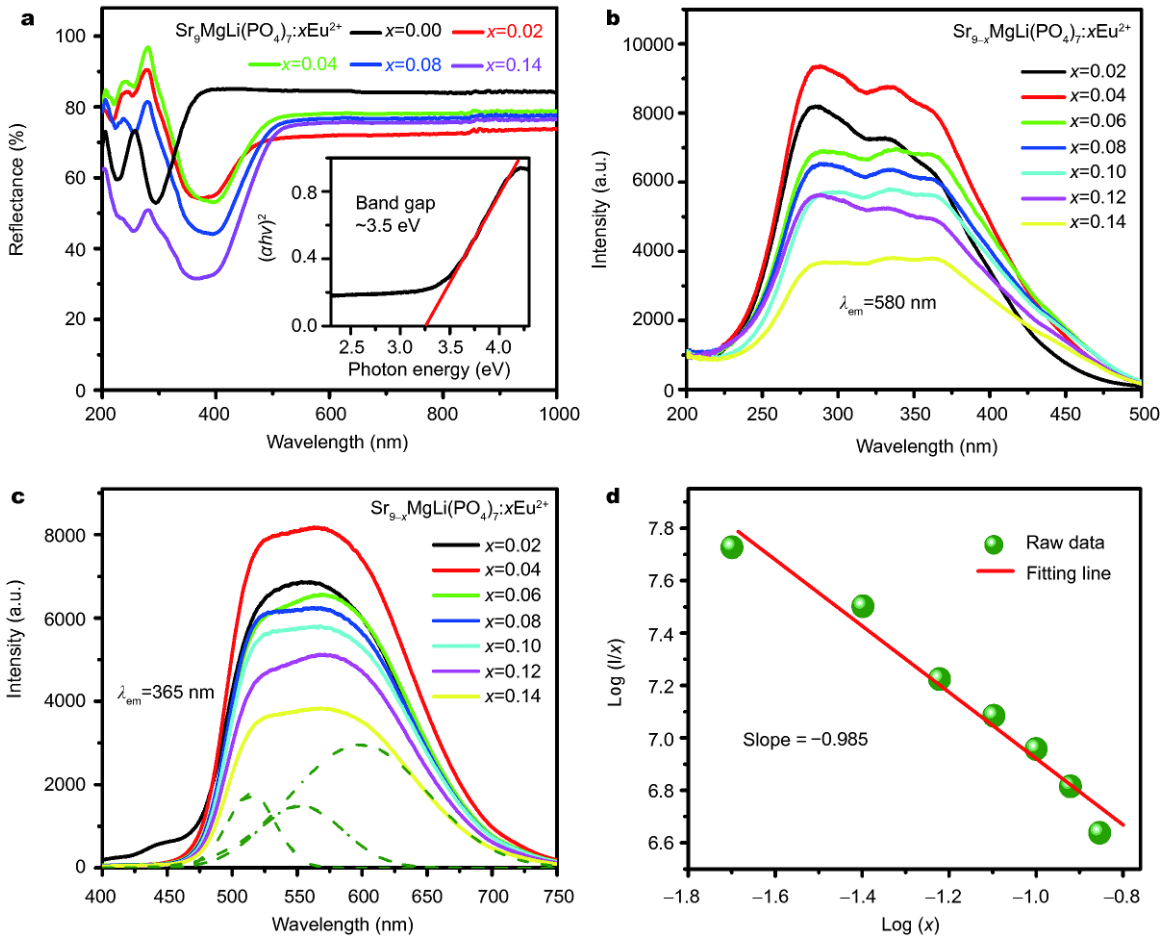

Figure 3 Absorption spectra of $Sr_{9-x}MgLi(PO_4)_7:xEu^{2+}$ (x = 0, 0.02, 0.04, 0.08, 0.14) and calculated energy gap by Tauc equation (a), PLE (b) and PL (c) spectra of $Sr_{9-x}MgLi(PO_4)_7:xEu^{2+}$ ($0.02 \le x \le 0.14$) phosphors, and the relationship between log(x) and log(I/x) in the $Sr_{9-x}MgLi(PO_4)_7:xEu^{2+}$ phosphors (d).

culated to be 21.67 Å. Thus, the energy transfer among Eu^{2+} ions in $Sr_{9-x}MgLi(PO_4)_7:xEu^{2+}$ phosphors is not triggered by the exchange interaction type since the corresponding critical distance for exchange interaction is about 3–5 Å [31]. According to Dexter's theory, the type of electric multipolar interaction can be calculated by using the following formula [32]:

$$I/x = K[1+\beta(x)^{\theta/3}]^{-1}, \quad (2)$$

where I is the integrated emission intensity, x is the activator concentration, K and β are constants for the same excitation condition for a given host lattice; θ=3 stands for energy transfer among the nearest neighbor ions, while θ=6, 8 and 10 stands for dipole-dipole, dipole-quadrupole and quadrupole-quadrupole interactions, respectively. Fig. 3d shows that the relationship of log(I/x) *vs.* log(x) is linear and the slope is −0.985. Thus, the value of θ was calculated to be 2.955, which is approximately equal to 3, indicating that the energy transfer among the nearest neighbor ions dominates the concentration quenching of the Eu^{2+} emission in the $Sr_9MgLi(PO_4)_7:Eu^{2+}$ phosphors [33].

Fluorescence lifetime properties

Fig. 4 presents decay curves of $Sr_{9-x}MgLi(PO_4)_7:xEu^{2+}$ ($0.02 \le x \le 0.14$) phosphors under excitation at 365 nm, monitored at the peak of 560 nm at room temperature. The corresponding luminescent decay curves could be fitted using a bi-exponential temporal dependence according to Equation 3 [9]:

$$I = A_1\exp\left(-\frac{t}{\tau_1}\right) + A_2\exp\left(-\frac{t}{\tau_2}\right), \quad (3)$$

where I is the luminescence intensity, t is the time after

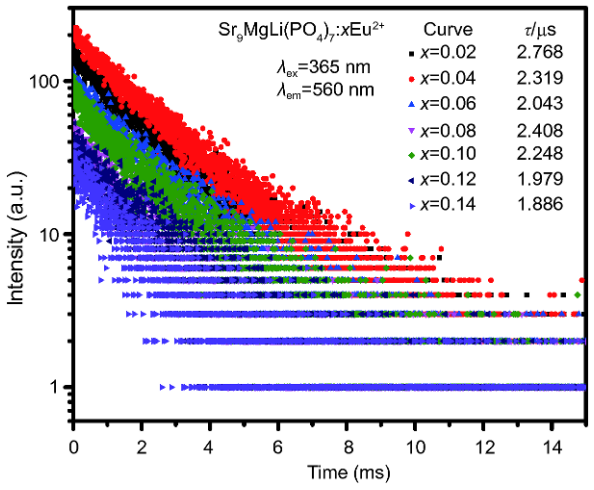

Figure 4 The decay curves of the Eu^{2+} emission in $Sr_{9-x}MgLi(PO_4)_7$:xEu^{2+} ($0.02 \le x \le 0.14$) under excitation at 365 nm, monitored at 560 nm.

excitation, and τ_i (i=1, 2) is the decay time of the i component, A_1 and A_2 are constants. Using these parameters, the average decay time t can be calculated by the following formula:

$$I = \left(A_1\tau_1^2 + A_2\tau_2^2\right) / \left(A_1\tau_1 + A_2\tau_2\right). \quad (4)$$

With an increase in the Eu^{2+} concentration, the decay times gradually decrease from 2.768 to 1.886 μs, which directly demonstrates that energy transfer occurs among Eu^{2+} ions.

Thermal stability of $Sr_9MgLi(PO_4)_7:Eu^{2+}$ phosphor

Generally, thermal stability is an important character for phosphors applied in WLEDs. Fig. 5a shows the temperature-dependent PL spectra and integrated emission intensity (the inset) of the $Sr_{8.96}MgLi(PO_4)_7$:$0.04Eu^{2+}$ phosphor under 365 nm excitation. Obviously, the emission intensity decreases with an increase in temperature from 30°C to 300°C, and about 50% emission intensity remains when temperature raise up to 150°C. To explain the thermal behavior of $Sr_{8.96}MgLi(PO_4)_7$:$0.04Eu^{2+}$, the activation energy (ΔE) is obtained from the following formula [31]:

$$I_T = \frac{I_0}{1 + A\exp\left(-\frac{\Delta E}{kT}\right)}, \quad (5)$$

where I_0 and I_T is the initial PL intensity of the phosphor at room and experimental temperature, A is a constant, k is the Boltzmann constant (k = 8.617×10^{-5} eV K^{-1}). By linear fitting the relationship of $\ln[(I_0/I_T)-1]$ *vs.* $1/kT$, the value of ΔE is about 0.282 eV, as shown in Fig. 5b. The high value of ΔE (compared with Chen's report [34]) indicates that $Sr_9MgLi(PO_4)_7:Eu^{2+}$ phosphor can serve as a potential yellow-emitting phosphor in UV chips based WLED applications.

Electroluminescence properties

The CIE chromaticity coordinates of $Sr_9MgLi(PO_4)_7:Eu^{2+}$ phosphor and digital images upon 365 nm UV light excitation are shown in Fig. 6a. $Sr_9MgLi(PO_4)_7:Eu^{2+}$ takes on homogeneous and bright yellow light, and the CIE coordinate is (0.518, 0.462). Furthermore, the internal quantum efficiency is measured to be 76%. All the above information indicates that $Sr_9MgLi(PO_4)_7:Eu^{2+}$ is suitable to be applied in UV chip pumped WLED. Based on this, we combined blue emitting $BaMgAl_{10}O_{17}:Eu^{2+}$ and yellow-

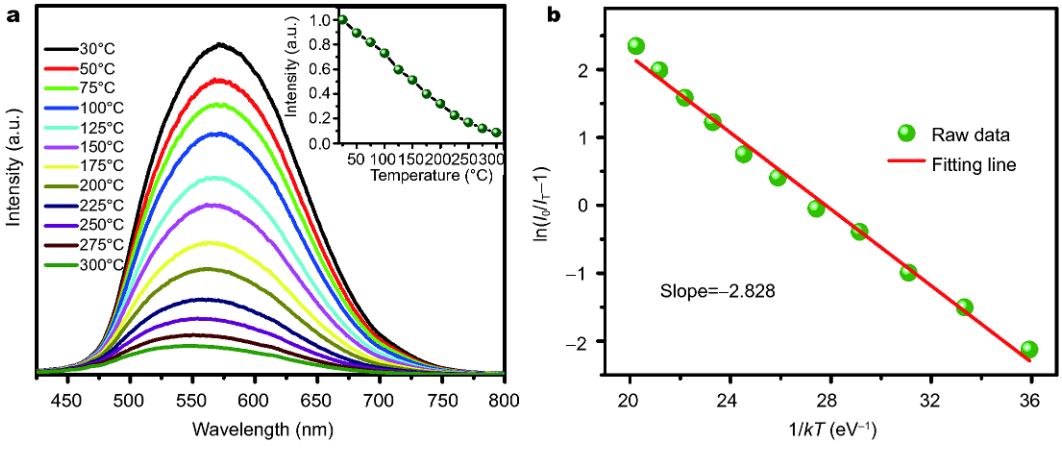

Figure 5 Temperature-dependent PL spectra of the selected $Sr_{8.96}MgLi(PO_4)_7$:$0.04Eu^{2+}$ phosphor, and inset shows the normalized emission intensity as a function of temperature (λ_{ex}=365 nm) (a), and Arrhenius fitting of the emission intensity of $Sr_{8.96}MgLi(PO_4)_7$:$0.04Eu^{2+}$ phosphor (b).

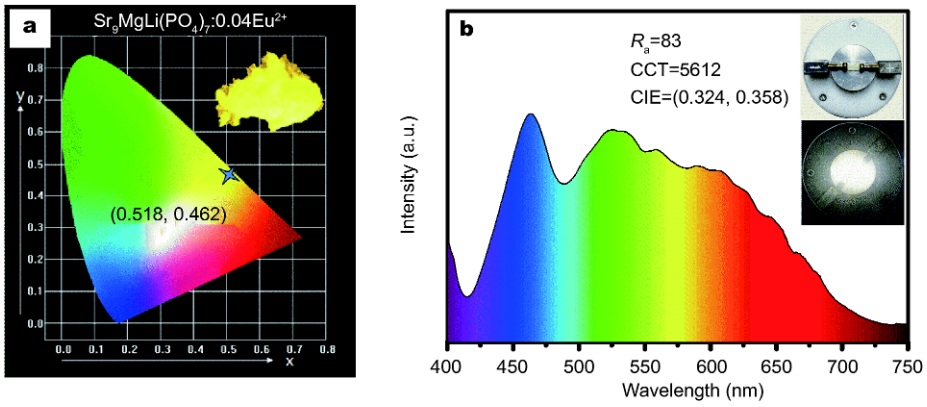

Figure 6 CIE coordinates and a digital photo of the selected $Sr_{8.96}MgLi(PO_4)_7$:0.04Eu^{2+} phosphor under 365 nm UV lamp (a), and electroluminescent spectrum of the fabricated WLED (b).

emitting $Sr_9MgLi(PO_4)_7$:Eu^{2+} with a commercial UV LED chips (λ=365 nm) to realize white light emitting. The corresponding CRI, CCT, and CIE chromaticity coordinates of the WLED device were found to be 83, 5,612 K, and (0.324, 0.358), respectively, as shown in Fig. 6b. The WLED packaging results demonstrate that $Sr_9MgLi(PO_4)_7$:Eu^{2+} is a great potential candidate as UV-excitable white emitting phosphor.

CONCLUSIONS

In summary, new $Sr_9MgLi(PO_4)_7$:Eu^{2+} phosphors have been successfully synthesized by the high temperature solid-state reaction method. $Sr_9MgLi(PO_4)_7$:Eu^{2+} possess a β-$Ca_3(PO_4)_2$-type structure with space group of *R3c*, and the lattice parameters are a=b=10.608 Å, c=39.356 Å, α=β=90°, γ=120°, Z=2, V=3,835.269 Å^3. Upon 365 nm UV light excitation, the $Sr_9MgLi(PO_4)_7$:Eu^{2+} phosphor exhibits a broad emission band from 450 to 700 nm, which are ascribed to the 5d-4f transitions of Eu^{2+}. The as-fabricated WLED device gives a high CRI (R_a = 83), indicating that $Sr_9MgLi(PO_4)_7$:Eu^{2+} phosphor might be promising as a candidate for UV WLED lamp.

Received 28 November 2017; accepted 03 January 2018; published online 25 January 2018

1 Luo W, Liu Y, Chen X. Lanthanide-doped semiconductor nanocrystals: electronic structures and optical properties. Sci China Mater, 2015, 58: 819–850
2 Huang P, Tu D, Zheng W, *et al.* Inorganic lanthanide nanoprobes for background-free luminescent bioassays. Sci China Mater, 2015, 58: 156–177
3 Wang D, Wang R, Liu L, *et al.* Down-shifting luminescence of water soluble $NaYF_4$:Eu^{3+}@Ag core-shell nanocrystals for fluorescence turn-on detection of glucose. Sci China Mater, 2017, 60: 68–74
4 Xia Z, Liu Q. Progress in discovery and structural design of color conversion phosphors for LEDs. Prog Mater Sci, 2016, 84: 59–117
5 Xia Z, Liu G, Wen J, *et al.* Tuning of photoluminescence by cation nanosegregation in the $(CaMg)_x(NaSc)_{1-x}Si_2O_6$ solid solution. J Am Chem Soc, 2016, 138: 1158–1161
6 Pimputkar S, Speck JS, Denbaars SP, *et al.* Prospects for LED lighting. Nat Photonics, 2009, 3: 180–182
7 Zhao M, Xia Z, Molokeev MS, *et al.* Temperature and Eu^{2+}-doping induced phase selection in $NaAlSiO_4$ polymorphs and the controlled yellow/blue emission. Chem Mater, 2017, 29: 6552–6559
8 Bachmann V, Ronda C, Meijerink A. Temperature quenching of yellow Ce^{3+} luminescence in YAG:Ce. Chem Mater, 2009, 21: 2077–2084
9 Xia Z, Zhang Y, Molokeev MS, *et al.* Structural and luminescence properties of yellow-emitting $NaScSi_2O_6$:Eu^{2+} phosphors: Eu^{2+} site preference analysis and generation of red emission by codoping Mn^{2+} for white-light-emitting diode applications. J Phys Chem C, 2013, 117: 20847–20854
10 Xia Y, Chen J, Liu Y, *et al.* Crystal structure evolution and luminescence properties of color tunable solid solution phosphors $Ca_{2+x}La_{8-x}(SiO_4)_{6-x}(PO_4)_xO_2$:$Eu^{2+}$. Dalton Trans, 2016, 45: 1007–1015
11 Huang L, Zhu Y, Zhang X, *et al.* HF-free hydrothermal route for synthesis of highly efficient narrow-band red emitting phosphor $K_2Si_{1-x}F_6$:xMn^{4+} for warm white light-emitting diodes. Chem Mater, 2016, 28: 1495–1502
12 Xuan T, Yang X, Lou S, *et al.* Highly stable $CsPbBr_3$ quantum dots coated with alkyl phosphate for white light-emitting diodes. Nanoscale, 2017, 9: 15286–15290
13 Ji H, Huang Z, Xia Z, *et al.* Discovery of new solid solution phosphors *via* cation substitution-dependent phase transition in $M_3(PO_4)_2$:Eu^{2+} (M = Ca/Sr/Ba) quasi-binary sets. J Phys Chem C, 2015, 119: 2038–2045
14 Xia Z, Liu H, Li X, *et al.* Identification of the crystallographic sites of Eu^{2+} in $Ca_9NaMg(PO_4)_7$: structure and luminescence properties study. Dalton Trans, 2013, 42: 16588–16595
15 Chen M, Xia Z, Molokeev MS, *et al.* Probing Eu^{2+} luminescence from different crystallographic sites in $Ca_{10}M(PO_4)_7$:Eu^{2+} (M = Li, Na, and K) with β-$Ca_3(PO_4)_2$-type structure. Chem Mater, 2017, 29: 7563–7570

16 Morozov VA, Belik AA, Kotov RN, *et al.* Crystal structures of double calcium and alkali metal phosphates $Ca_{10}M(PO_4)_7$ (M = Li, Na, K). Crystallogr Rep, 2000, 45: 13–20
17 Wang J, Zhang Z, Zhang M, *et al.* The energy transfer from Eu^{2+} to Tb^{3+} in $Ca_{10}K(PO_4)_7$ and its application in green light emitting diode. J Alloys Compd, 2009, 488: 582–585
18 Zhao J, Wu Y, Liang Y, *et al.* A novel green-emitting phosphor $Ca_{10}Na(PO_4)_7$:Eu^{2+} for near ultraviolet white light-emitting diodes. Optical Mater, 2013, 35: 1675–1678
19 Wang Y, Li H, Zhang R, *et al.* Investigations on the luminescence of emission-tunable $Ca_{10}K(PO_4)_7$:Eu^{2+}, Sr^{2+}, Mg^{2+} phosphors for white LEDs. RSC Adv, 2015, 5: 2689–2693
20 Huang CH, Chen TM. $Ca_9La(PO_4)_7$:Eu^{2+},Mn^{2+}: an emission-tunable phosphor through efficient energy transfer for white light-emitting diodes. Opt Express, 2010, 18: 5089–5099
21 Guo N, You H, Song Y, *et al.* White-light emission from a single-emitting-component $Ca_9Gd(PO_4)_7$:Eu^{2+},Mn^{2+} phosphor with tunable luminescent properties for near-UV light-emitting diodes. J Mater Chem, 2010, 20: 9061–9067
22 Huang CH, Chen TM, Liu WR, *et al.* A single-phased emission-tunable phosphor $Ca_9Y(PO_4)_7$:Eu^{2+},Mn^{2+} with efficient energy transfer for white-light-emitting diodes. ACS Appl Mater Interfaces, 2010, 2: 259–264
23 Guo N, Huang Y, You H, *et al.* $Ca_9Lu(PO_4)_7$:Eu^{2+},Mn^{2+}: a potential single-phased white-light-emitting phosphor suitable for white-light-emitting diodes. Inorg Chem, 2010, 49: 10907–10913
24 Xie F, Li J, Dong Z, *et al.* Energy transfer and luminescent properties of $Ca_8MgLu(PO_4)_7$:Tb^{3+}/Eu^{3+} as a green-to-red color tunable phosphor under NUV excitation. RSC Adv, 2015, 5: 59830–59836
25 Xue YN, Xiao F, Zhang QY. A red-emitting $Ca_8MgLa(PO_4)_7$:Ce^{3+}, Mn^{2+} phosphor for UV-based white LEDs application. Spectrochim Acta Part A-Mol Biomol Spectr, 2011, 78: 1445–1448
26 Huang Y, Ding H, Jang K, *et al.* Luminescence properties of triple phosphate $Ca_8MgGd(PO_4)_7$:Eu^{2+} for white light-emitting diodes. J Phys D-Appl Phys, 2008, 41: 095110
27 Wang Y, Zhang J, Shi J, *et al.* Luminescence properties of $(Sr_{0.86}Mg_{0.14})_3(PO_4)_2$:$Eu^{2+}$,$Mn^{2+}$ phosphors for LEDs application. J Mater Sci-Mater Electron, 2017, 28: 8895–8900
28 Bruker A. TOPAS V3: General Profile and Structure Analysis Software for Powder Diffraction Data. User's Manual, Karlsruhe: Bruker AXS, 2005
29 Zhou J, Xia Z, Molokeev MS, *et al.* Composition design, optical gap and stability investigations of lead-free halide double perovskite $Cs_2AgInCl_6$. J Mater Chem A, 2017, 5: 15031–15037
30 Blasse G. Energy transfer between inequivalent Eu^{2+} ions. J Solid State Chem, 1986, 62: 207–211
31 Xia Z, Liu RS, Huang KW, *et al.* $Ca_2Al_3O_6F$:Eu^{2+}: a green-emitting oxyfluoride phosphor for white light-emitting diodes. J Mater Chem, 2012, 22: 15183–15189
32 Dexter DL. A theory of sensitized luminescence in solids. J Chem Phys, 1953, 21: 836–850
33 Zhang X, Zhou L, Pang Q, *et al.* Synthesis, photoluminescence and Judd–Ofelt analysis of red $LiGd_5P_2O_{13}$:Eu^{3+} phosphors for white LEDs. RSC Adv, 2015, 5: 54622–54628
34 Chen M, Xia Z, Molokeev MS, *et al.* Tuning of photoluminescence and local structures of substituted cations in $xSr_2Ca(PO_4)_2$–$(1–x)Ca_{10}Li(PO_4)_7$:Eu^{2+} phosphors. Chem Mater, 2017, 29: 1430–1438

Acknowledgements The present work was supported by the National Natural Science Foundation of China (51722202, 91622125 and 51572023) and Natural Science Foundation of Beijing (2172036).

Author contributions Xia Z designed and engineered the samples; Qiao J, Zhang Z and Hu B performed the experiments; Qiao J wrote the paper with support from Xia Z and Liu Q. All authors contributed to the general discussion.

Conflict of interest The authors declare no conflict of interest.

Jianwei Qiao is a PhD student in the University of Science and Technology Beijing. He completed his bachelor degree at Taiyuan Normal University in 2014 and received the master degree from Taiyuan University of Technology in 2017. His research is mainly focused on the rare earth ions activated phosphate luminescent materials for white LEDs.

Zhiguo Xia is a professor of materials chemistry and physics in the University of Science and Technology Beijing (USTB). He obtained his bachelor degree in 2002 and master degree in 2005 from Beijing Technology and Business University, and he received his PhD degree from Tsinghua University in 2008. Since then he has been working as an assistant and associate Professor in China University of Geosciences, Beijing (CUGB), 2008-2014. After that, he joined USTB as a full professor. His research interests are in designing of new rare earth phosphors for white LED by integrating structural discovery, modification and structure-property relation studies.

近紫外芯片激发的白光LED用黄色荧光粉$Sr_9MgLi(PO_4)_7:Eu^{2+}$

乔建伟, 夏志国*, 张志超, 胡彬涛, 刘泉林

摘要 发现新型白光LED用荧光粉一直是材料科学领域一项重要的挑战. 采用本课题组提出的矿物结构模型, 高效设计了稀土发光材料新物相, 并解析、确定新物相的晶体结构. 本论文用黄色荧光粉$Sr_9MgLi(PO_4)_7:Eu^{2+}$设计合成了一种新型白光LED, 并对其结构和发光特性进行了分析表征. 研究发现: 其物相结构是源于β-$Ca_3(PO_4)_2$矿物模型. 在365 nm近紫外光激发下, $Sr_9MgLi(PO_4)_7:Eu^{2+}$呈现出一个从450 nm到700 nm的宽带发射. 通过把$Sr_9MgLi(PO_4)_7:Eu^{2+}$黄粉与商用蓝粉$BaMgAl_{10}O_{17}:Eu^{2+}$混合涂敷在蓝光芯片表面, 制作得到了白光LED器件. 测试结果显示, LED的R_a, CCT, CIE值分别为83, 5612 K, (0.324, 0.358), 表明$Sr_9MgLi(PO_4)_7:Eu^{2+}$可作为白光LED用黄光荧光粉.

